*Assemblée Générale GdR APPEL, Talence, 11-13 Mai 2022*

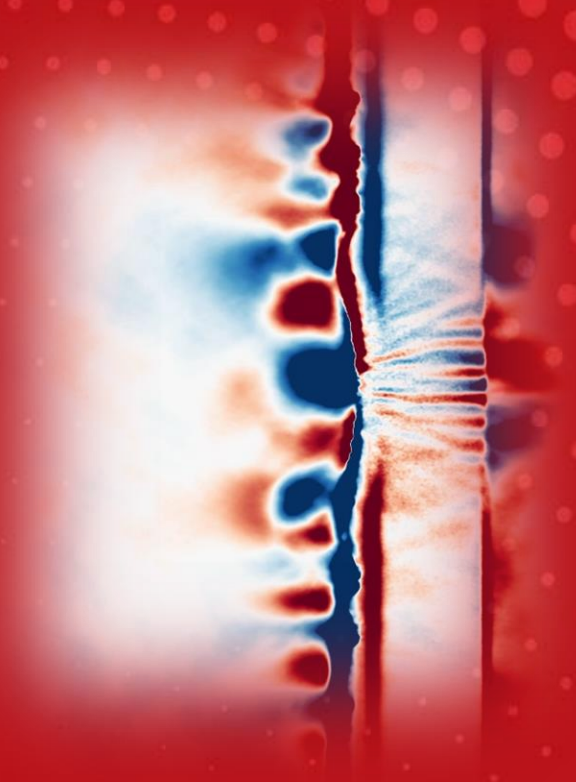

# Atomic physics modeling in the CALDER PIC code

D. Tordeux, L. Gremillet, C. Blancard, X. Davoine

*CEA, DAM, DIF, 91297 Arpajon, France*

*Université Paris-Saclay, CEA, LMCE, 91680 Bruyères-le-Châtel, France*

# CALDER: a versatile PIC code developed at CEA/DAM for kinetic plasma simulations in a wide range of physical settings

Laser-plasma electron accelerators

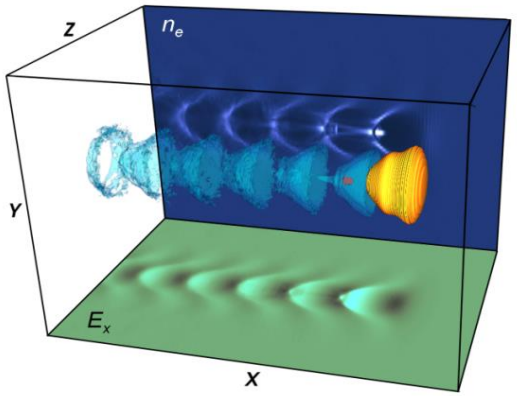


Laser generation of HED matter

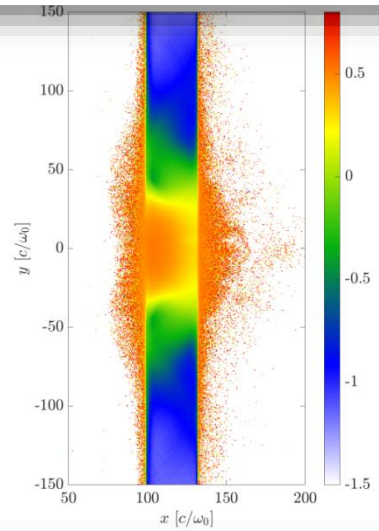


Laser-driven on acceleration

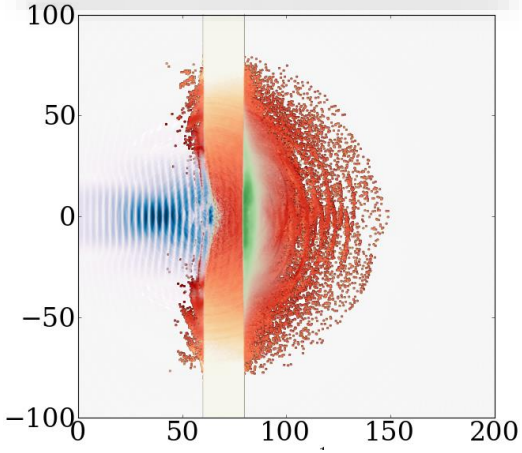

Strong B-field generation, Laboratory astrophysics

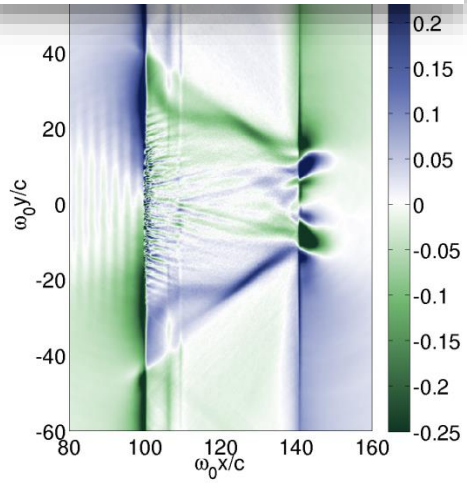


High-energy photon and pair production, strong-field physics

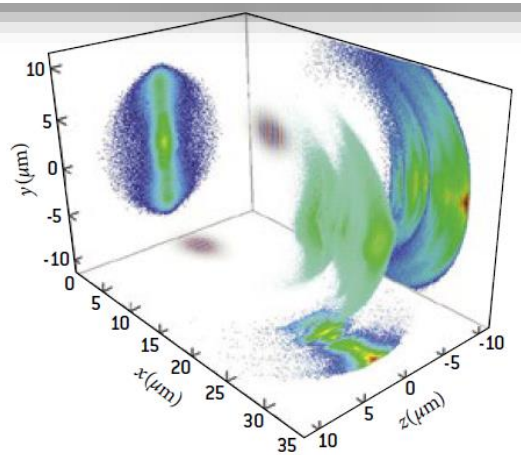


Laser-driven terahertz sources

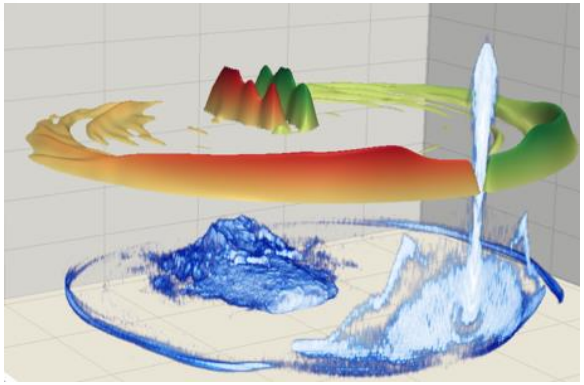

# Motivation for an atomic physics capability in PIC codes

- PIC codes are specifically designed the kinetics of collisionless plasmas by modeling them as aggregates of macro-particles, i.e., clusters of neighboring real particles in phase space.
- At high plasma densities and/or relatively low temperatures, inter-particle interactions play an important role in the energy/momentum transfers between the plasma populations. Such is the case for solid-density plasmas irradiated by intense laser or x-ray pulses.
- Inter-particle (or photon-particle) interactions are intrinsically of stochastic character, and so readily lend themselves to the Monte Carlo method.

# Motivation for an atomic physics capability in PIC codes

- PIC codes are specifically designed the kinetics of collisionless plasmas by modeling them as aggregates of macro-particles, i.e., clusters of neighboring real particles in phase space.
- At high plasma densities and/or relatively low temperatures, inter-particle interactions play an important role in the energy/momentum transfers between the plasma populations. Such is the case for solid-density plasmas irradiated by intense laser or x-ray pulses.
- Inter-particle (or photon-particle) interactions are intrinsically of stochastic character, and so readily lend themselves to the Monte Carlo method.
- List of atomic and radiative processes now implemented in CALDER
  - Coulomb collisions[1,2]
  - Collisional ionization[1,2]
  - Atomic deexcitation[2]
  - Three-body recombination[2]
  - Ionization potential depression[2]
  - Photoionization[2]
  - Radiative recombination[2]
  - Compton scattering[2]
  - Bremsstrahlung[3]
  - Synchrotron radiation[4]
  - Bethe-Heitler pair production[3]
  - Breit-Wheeler pair production[4]

[1]F. Pérez *et al.,* Phys. Plasmas **19**, 83104 (2012).
[2]D. Tordeux, Thèse de doctorat de l'Université Paris-Saclay (2022).
[3]B. Martinez *et al.,* Phys. Plasmas **26**, 103109 (2019).
[4]M. Lobet *et al.*, J. Phys.: Conf. Ser. **688**, 012058 (2016).

# Motivation for an atomic physics capability in PIC codes

- PIC codes are specifically designed the kinetics of collisionless plasmas by modeling them as aggregates of macro-particles, i.e., clusters of neighboring real particles in phase space.
- At high plasma densities and/or relatively low temperatures, inter-particle interactions play an important role in the energy/momentum transfers between the plasma populations. Such is the case for solid-density plasmas irradiated by intense laser or x-ray pulses.
- Inter-particle (or photon-particle) interactions are intrinsically of stochastic character, and so readily lend themselves to the Monte Carlo method.
- List of atomic and radiative processes now implemented in CALDER
  - Coulomb collisions[1,2]
  - Collisional ionization[1,2]
  - Atomic deexcitation[2]
  - Three-body recombination[2]
  - Ionization potential depression[2]
  - Photoionization[2]
  - Radiative recombination[2]
  - Compton scattering[2]
  - Bremsstrahlung[3]
  - Synchrotron radiation[4]
  - Bethe-Heitler pair production[3]
  - Breit-Wheeler pair production[4]

[1]F. Pérez *et al.,* Phys. Plasmas **19**, 83104 (2012).
[2]D. Tordeux, Thèse de doctorat de l'Université Paris-Saclay (2022).
[3]B. Martinez *et al.,* Phys. Plasmas **26**, 103109 (2019).
[4]M. Lobet *et al.*, J. Phys.: Conf. Ser. **688**, 012058 (2016).

# Improved Monte Carlo collisional ionization resolved on the fine electron shell structure

- Based on relativistic electron impact ionization cross sections computed by Kim *et al.*[1]
- Original implementation of collisional ionization (CI) in CALDER used ionization probabilities averaged over atomic electron shells.[2]
- New implementation employs the same Monte Carlo technique, valid for arbitrary macro-particle weights[3], yet now resolves the $(n, l, j)$ electron shell structure.

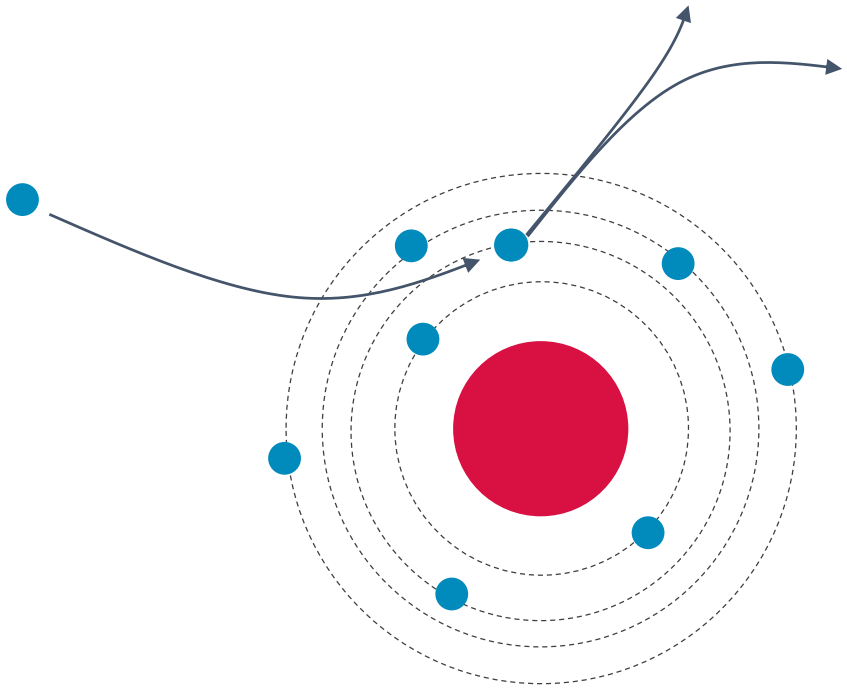

*Mean energy of liberated electron: Theory[1] vs Monte Carlo (CALDER) results*

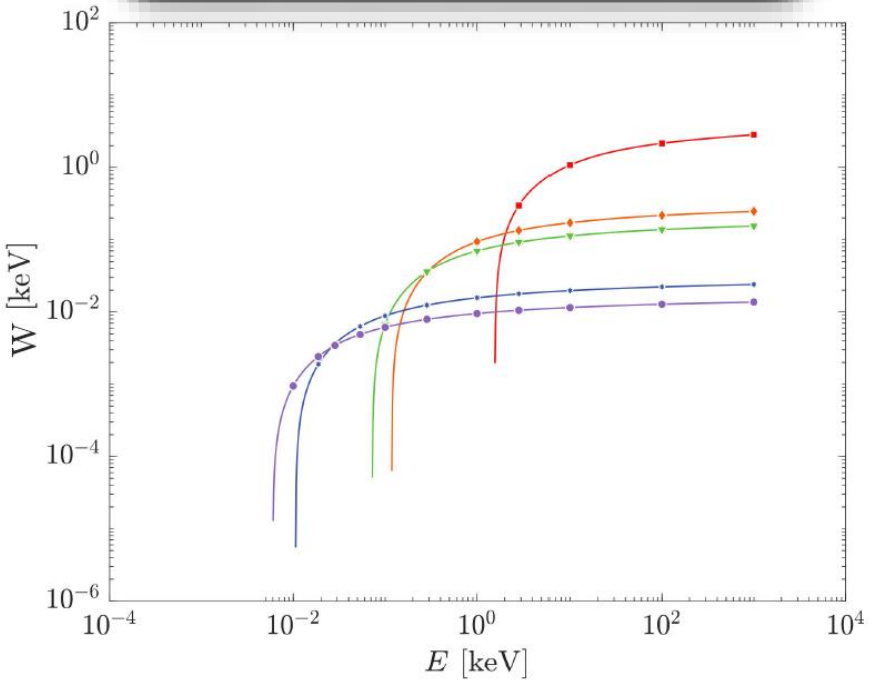


[1]Y.-K. Kim *et al.*, Phys. Rev. A **62**, 052710 (2000).
[2]F. Pérez *et al.,* Phys. Plasmas **19**, 083104 (2012).
[3]K. Nanbu and S. Yonemura, J. Comp. Phys. **145**, 639 (1998).

# Inverse process of collisional ionization: Three-body recombination

- TBR cross section obtained from relativistic CI cross section[1] through micro-reversibility relation:[2]

$$d\sigma^{\mathrm{TBR}}_{k,b\to a} = \frac{\pi^2\hbar^3}{\sqrt{2}m_e^{3/2}c}\frac{g_a}{g_b}\frac{\lambda(E)}{\lambda(E_1)\lambda(E_2)}\frac{\beta(E)}{\beta(E_1)\beta(E_2)}\frac{d\sigma^{\mathrm{CI}}_{k,a\to b}}{dE_1}$$

with $E_2 = E - E_1 - B_k$, $\lambda(E) = \sqrt{E(1+E/2m_ec^2)}(1+E/m_ec^2)$, $\beta = v/c$ and $g_\alpha$ the statistical weight of state $\alpha$.

- Monte Carlo approach considers an electron-ion pair immersed in an electron bath.
- Allows Saha-Boltzmann model's equilibrium predictions to be reproduced.

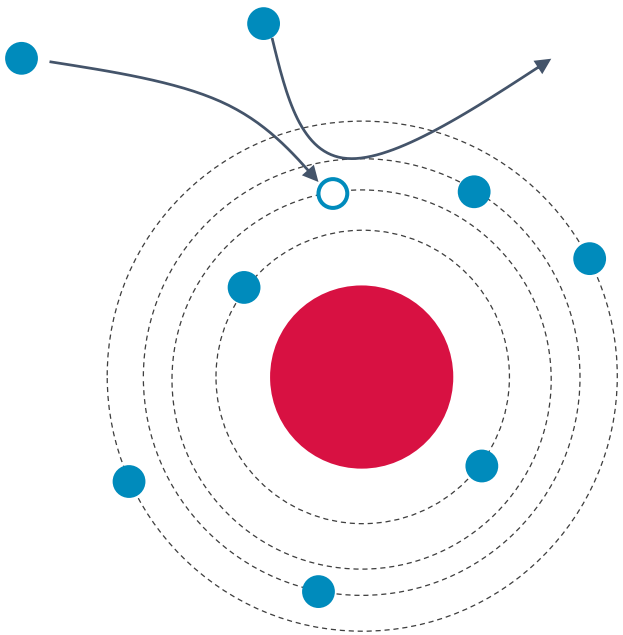

CALDER

*Equilibrium charge-state distribution of Al plasma at $T_e = 75\ eV$ and $\rho = 2.7\ gcm^{-3}$*

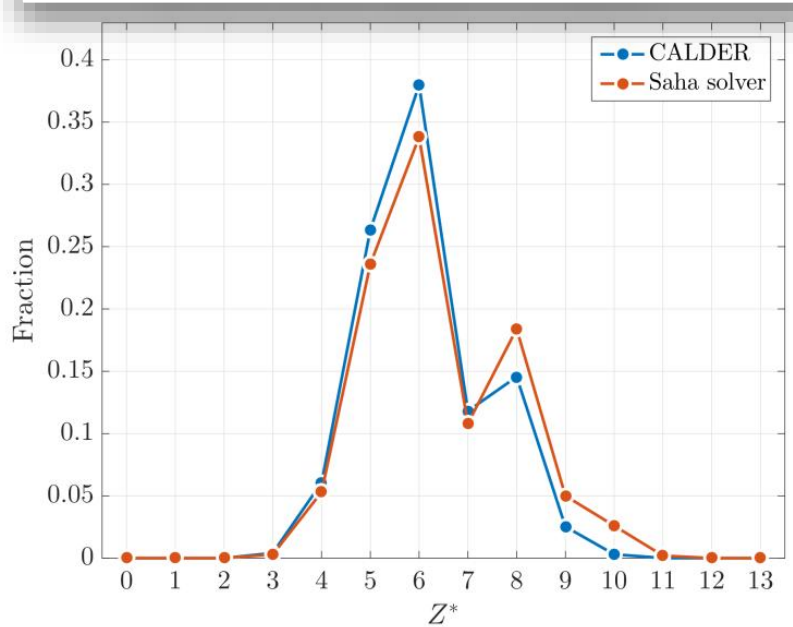


[1]Y.-K. Kim *et al.*, Phys. Rev. A **62**, 052710 (2000).
[2]G. Faussurier and C. Blancard, Phys. Rev. E **95**, 063201 (2017).

# Ionization potential depression in dense plasma environments

- Ions embedded in a plasma of free electrons and charged ions experience an electrostatic potential different from that seen by isolated ions.

  ⇒ This plasma-generated potential lowers the ionization threshold of bound states, with direct implications on collisional & field ionization and recombination rates in dense plasmas.
- Both Stewart & Pyatt[1] and Ecker-Kröll[2] models of IPD have been implemented.

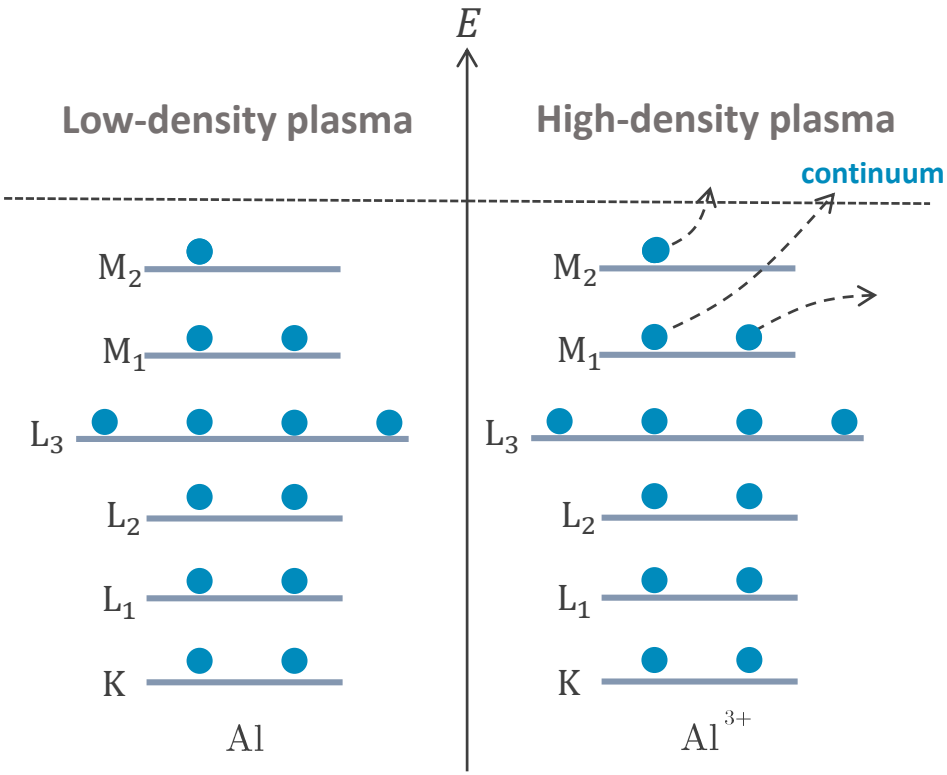


*Impact of IPD on equilibrium charge-state distribution of Al at $T_e = 50\ eV$ and $\rho = 2.7\ gcm^{-3}$*

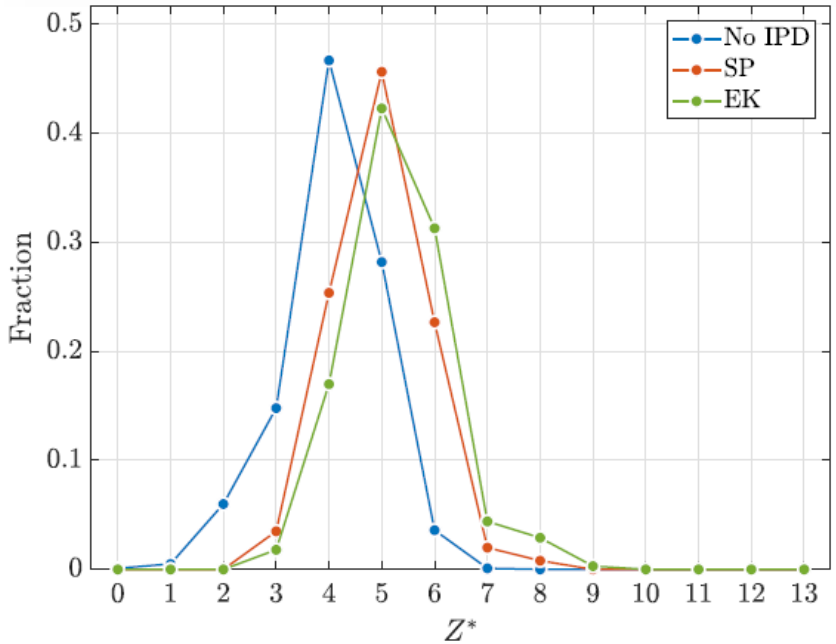


[1]J. C. Stewart and K. D. Pyatt, Astrophys. J. **144**, 1203 (1966).
[2]G. Ecker and W. Kröll, Phys. Fluids **6**, 62 (1963).

# Deexcitation cascades of atomic vacancies

- Monte Carlo module describes both radiative and nonradiative (Auger) transitions.

  ⇒ Ejection of several photons and electrons.
- Probability distributions of all liberated photons and electrons taken from Kaastra & Mewe's tabulations.[1]
- Limitations: only treats single atomic vacancies and assumes instantaneous deexcitation.

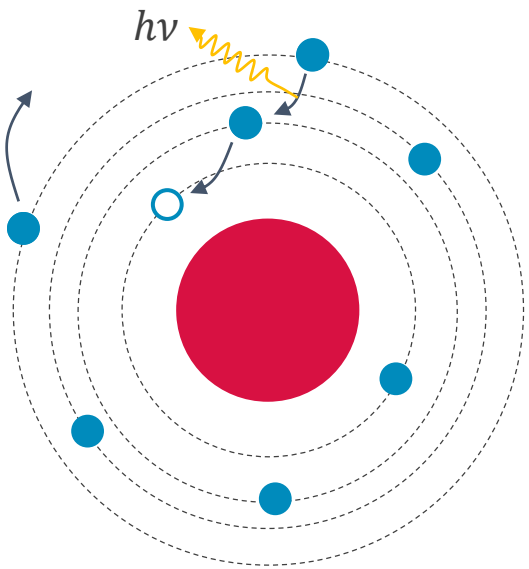


*Time evolution of $K$-shell x-ray emission spectrum from XFEL-Fe target interaction*

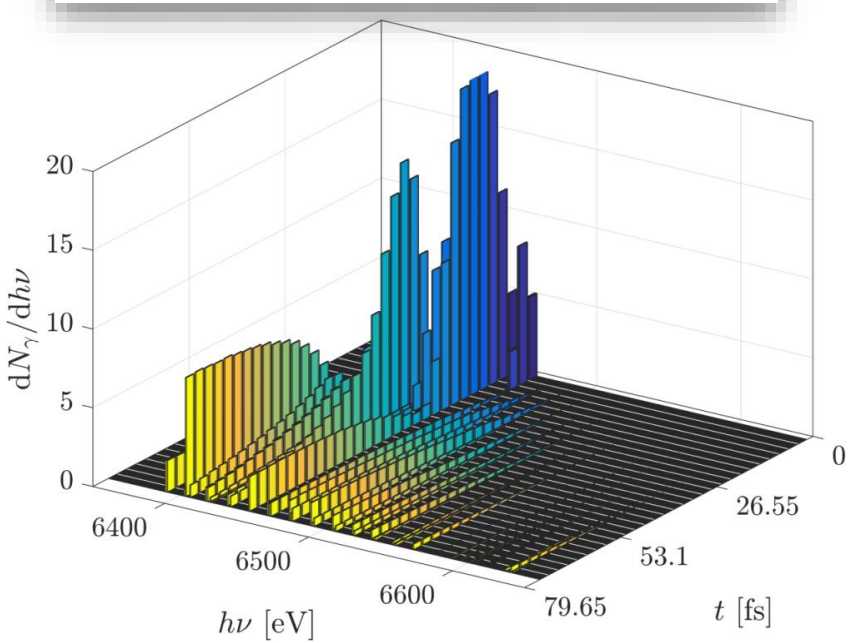


[1]J.-S. Kaastra and R. Mewe, Astron. Astrophys. Suppl. Ser. **97**, 443 (1993).

# Photoionization by x rays

- Cross sections computed using analytic fits derived by Verner and Yakovlev[1], valid for neutral and ionized atoms for $Z \leq 30$.
- Resolved on $(n, l)$ electron-shell structure.
- Monte Carlo results agree well with reference x-ray opacity database.[2]

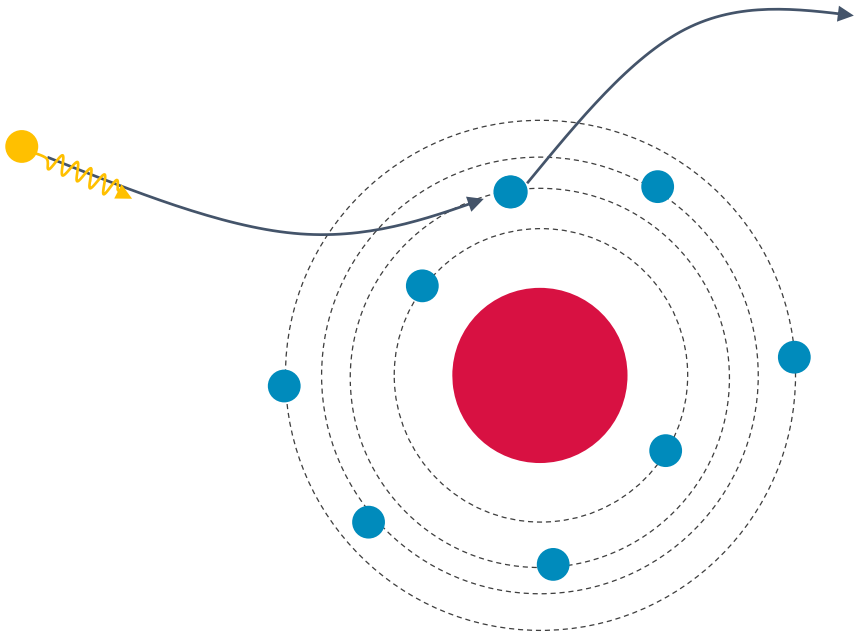

*Bound-free opacity of Al:*
*Monte Carlo (CALDER) results vs NIST data*

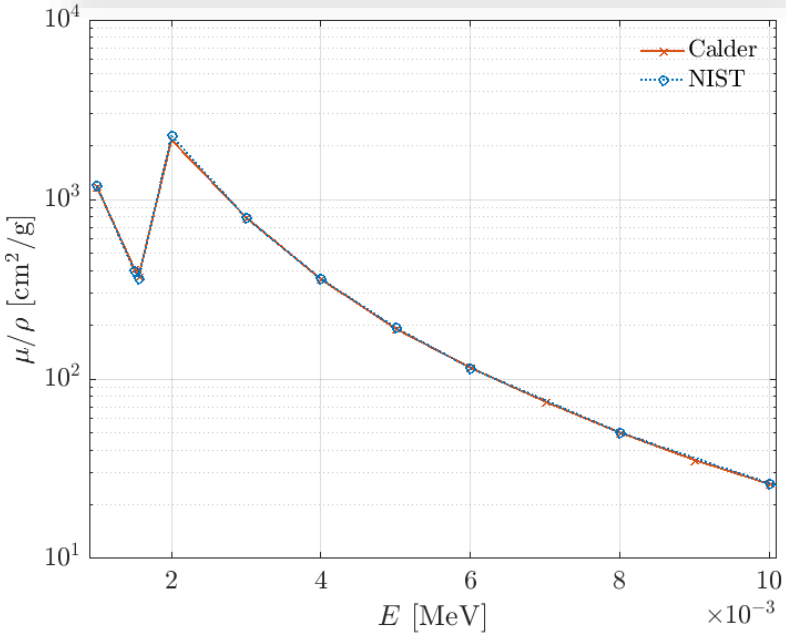


[1]D. A. Verner and D. G. Yakovlev ., Astron. Astrophys. Suppl. Ser. 109, 125 (1995).
[2]X-Ray mass attenuation coefficients, NIST Standard Reference Database.

# Inverse process of photoionization: Radiative recombination

- Cross section obtained from that of photoionization through micro-reversibility relation:[1]

$$\sigma^{\mathrm{RR}}_{k,b\to a}(E) = \frac{g_a}{g_b}\frac{(E+B_k)^2}{\sqrt{2}m_e^{3/2}c^3}\frac{\sigma^{\mathrm{PI}}_{k,a\to b}(E+B_k)}{\lambda(E)\beta(E)}$$

- Resolved on $(n, l)$ electron-shell structure.
- Contributes to background of x-ray emission spectrum.

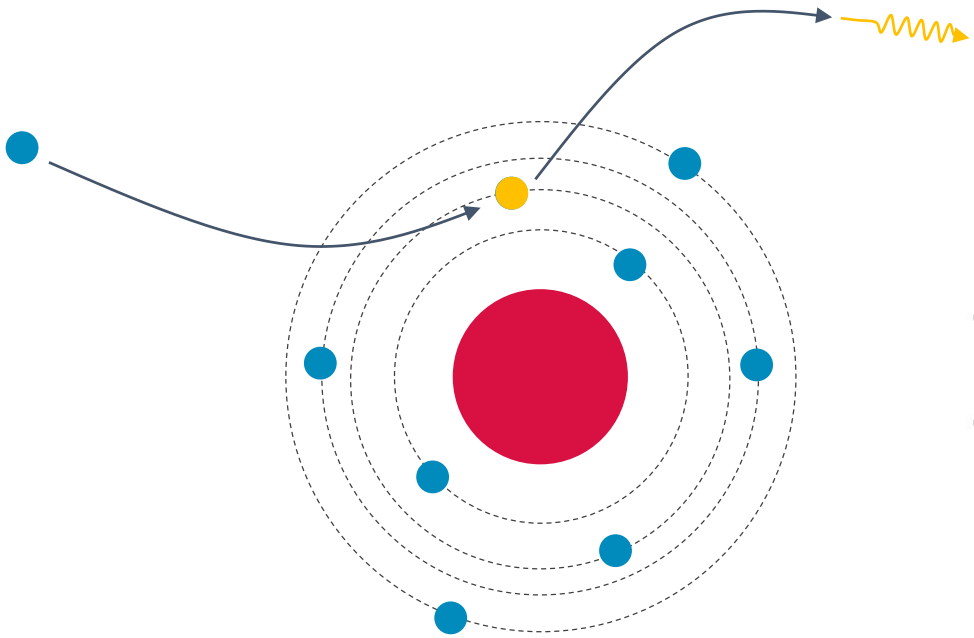

*Emission spectrum from Al solid target irradiated by ultraintense laser pulse*

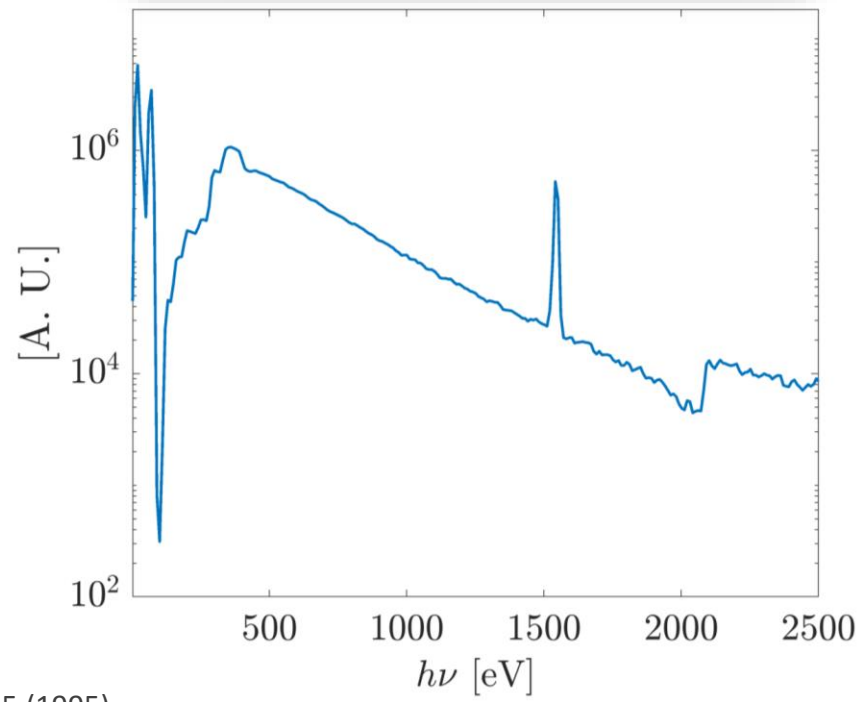


[1]G. Faussurier and C. Blancard, Phys. Rev. E **95**, 063201 (2017).
[2]D. A. Verner and D. G. Yakovlev ., Astron. Astrophys. Suppl. Ser. **109**, 125 (1995).

# Compton scattering of photons by free electrons

- Compton scattering described by Klein-Nishina cross section[1]:

$$\frac{d\sigma^*_{\mathrm{KN}}}{d\varepsilon^*} = \pi r_e^2 \frac{m_e c^2}{k^*}\left(\varepsilon^* + \frac{1}{\varepsilon^*}\right)\left(1 - \frac{\varepsilon^* \sin^2\theta^*}{1+\varepsilon^{*2}}\right)$$

- Monte Carlo algorithm implemented in CALDER uses rejection method to compute $\varepsilon^* = k_s^*/k^*$ and $\theta^*$ in the electron rest frame.[2]
- Properties of recoil electron deduced from energy and momentum conservation laws.

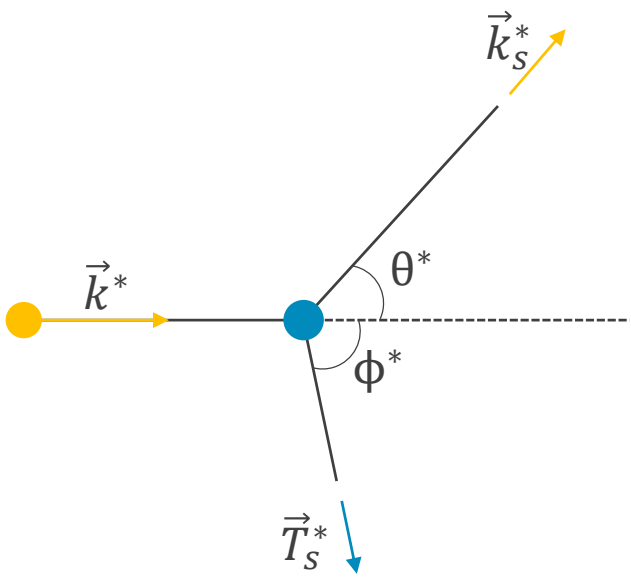


*Energy variation rate of a photon of energy $h\nu$ in a 100 $keV$ Maxwellian electron plasma: Monte Carlo (CALDER) vs theoretical[3] results*

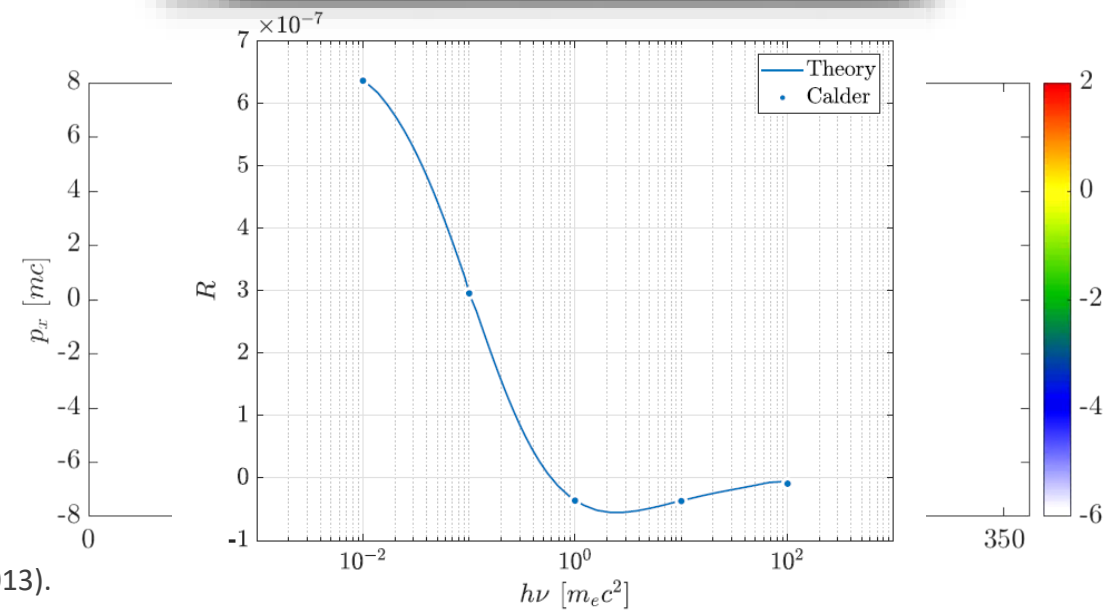


[1]O. Klein and Y. Nishina, Z. Med. Phys. **52**, 853 (1929).
[2]GEANT4 Collaboration, Physics Reference Manual (2013).
[3]A. Shestakov *et al.*, JQSRT **40**, 577 (1988).

# Macroparticle merging scheme

- Atomic physics modules may cause the number of macroparticles to grow rapidly

  ⇒ Need of a particle/photon merging scheme to reduce computational load.
- Implementation of merging scheme proposed by Vranic *et al.*[1]
- Macroparticles within each cell are projected onto a 3D momentum grid of mesh size scaled by local momentum spread.
- Particles within each momentum grid cell are coalesced to form two new particles of same weight and preserving momentum and energy conservation.

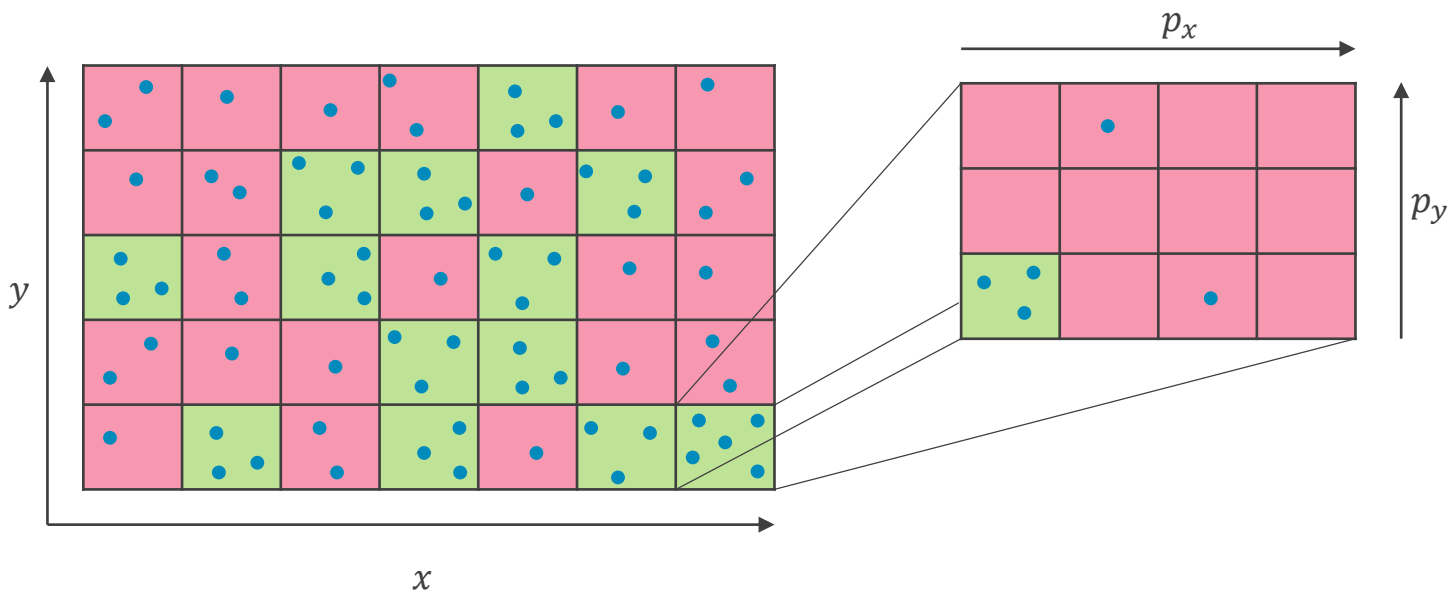


[1]M. Vranic *et al.*, Comput. Phys. Commun. **191**, 65 (2015).

# Macroparticle merging scheme

- Atomic physics modules may cause the number of macroparticles to grow rapidly

  ⇒ Need of a particle/photon merging scheme to reduce computational load.
- Implementation of merging scheme proposed by Vranic *et al.*[1]
- Macroparticles within each cell are projected onto a 3D momentum grid of mesh size scaled by local momentum spread.
- Particles within each momentum grid cell are coalesced to form two new particles of same weight and preserving momentum and energy conservation.

*Relaxation of an Al plasma with $T_e = T_i = 200\ eV$ and $\rho = 2.7\ gcm^{-3}$: Influence of execution period of particle merging scheme*

- Initial particle count/cell: $N_e = N_i = 200$.
- Momentum grid size: $\Delta p_{xyz} = \langle p_{th} \rangle / 5$.
- 50 000 time steps.

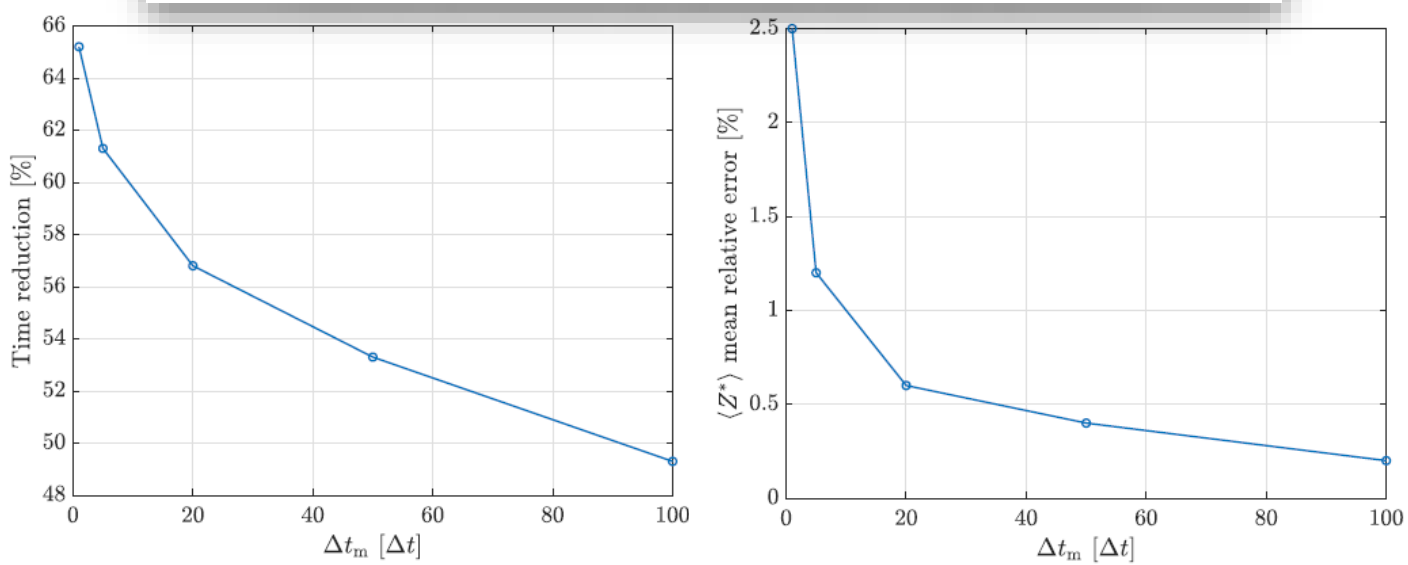


[1]M. Vranic *et al.*, Comput. Phys. Commun. **191**, 65 (2015).

# Benchmark against Saha-Boltzmann model: Stationary charge-state distributions of solid-density Al plasma

*Comparison between CALDER (solid) and Saha-Boltzmann (dotted) results.*

$T_e = 200$ eV – CI only

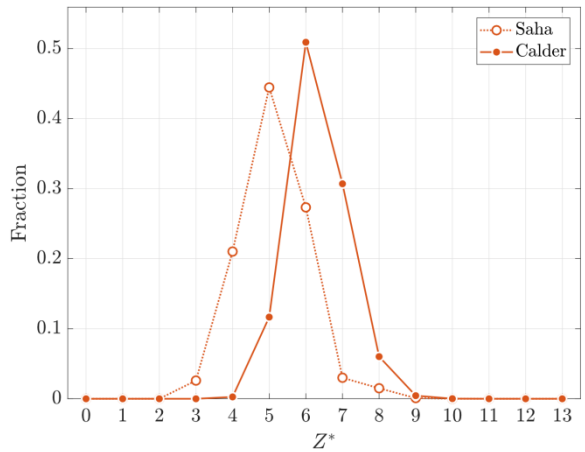


$T_e = 200$ eV – All processes

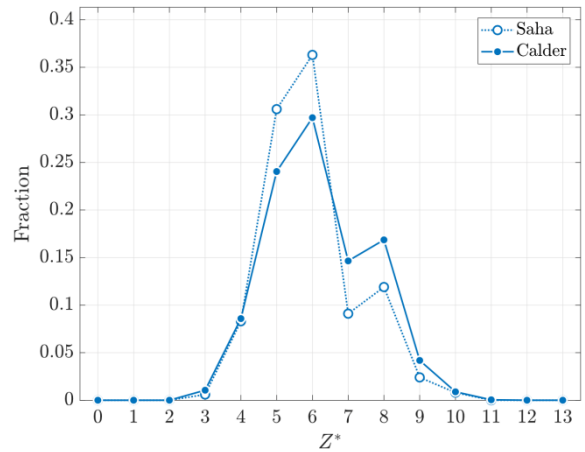


$T_e = 600$ eV – CI only

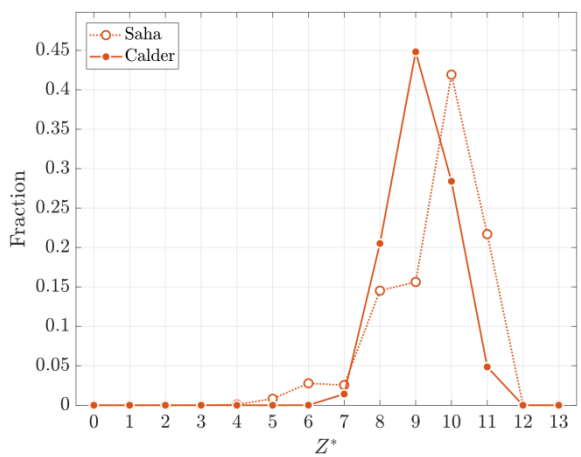


$T_e = 600$ eV – All processes

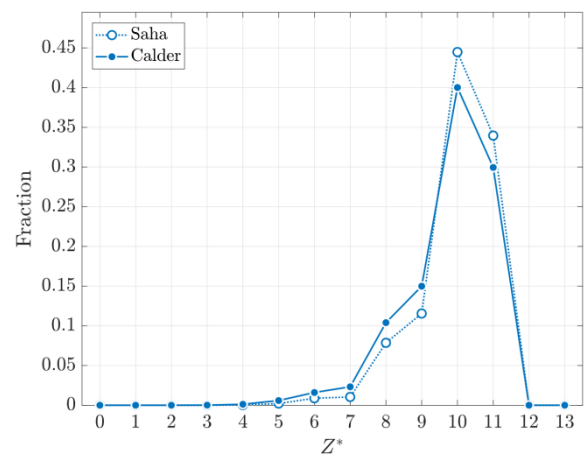

# Benchmark against FLYCHK atomic physics code[1]: Relaxation dynamics of nonequilibrium solid-density Al plasma

- Time-dependent, collisional-radiative FLYCHK code[1] fed with $T_e(t)$ and $T_i(t)$ recorded from CALDER simulation.
- Satisfactory agreement obtained between the two models.
- Initial faster rise in $\langle Z^* \rangle$ predicted by FLYCHK likely results from different collisional ionization cross sections (Lotz[2] vs Kim[3] formulas).

*Time evolution of mean ionization degree ($Z^*$) for a solid Al plasma initialized with $T_e = T_i = 200\ eV$ and $1\mathrm{keV}$ (right).*

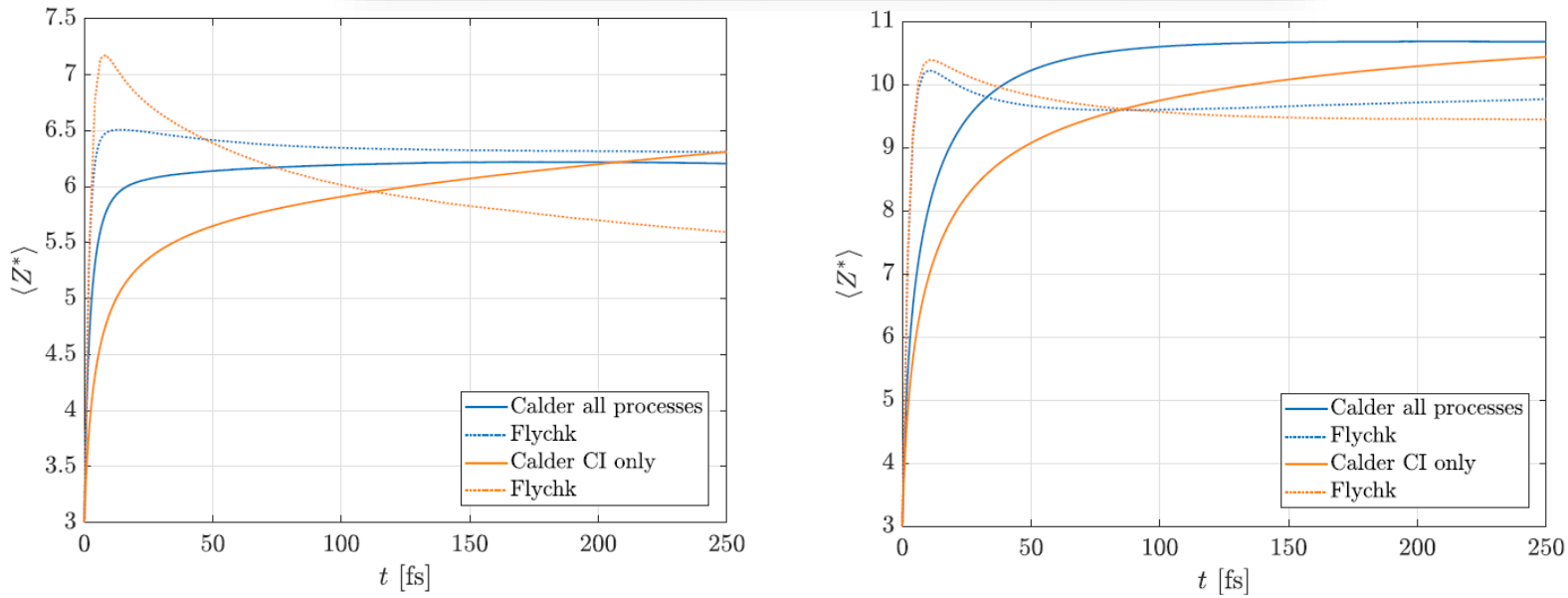


[1]H. K. Chung *et al.*, HEDP **1**, 3 (2005).
[2]W. Lotz, Z. Phys. A **232**, 101 (1970).
[3]Y.-K. Kim *et al.*, Phys. Rev. A **62**, 052710 (2000).

# Application to ultraintense laser-solid interactions

- Integrated simulation of a $1.36 \times 10^{20}\mathrm{Wcm}^{-2}$, 30 fs pulse with a 3 $\mu$m thick Al foil with a $\sim$ 2 $\mu$m scale length preplasma.
- Overall, accounting for all atomic physics processes leads to relatively weak changes to the heated target properties. However, compared to the CI only case, one obtains a significantly larger ionized region with slightly weaker ($\sim 0.5 - 1$ keV) temperatures.

*Mean ionization $\langle Z^* \rangle$ at $t = 130\ fs$ after the laser maximum*

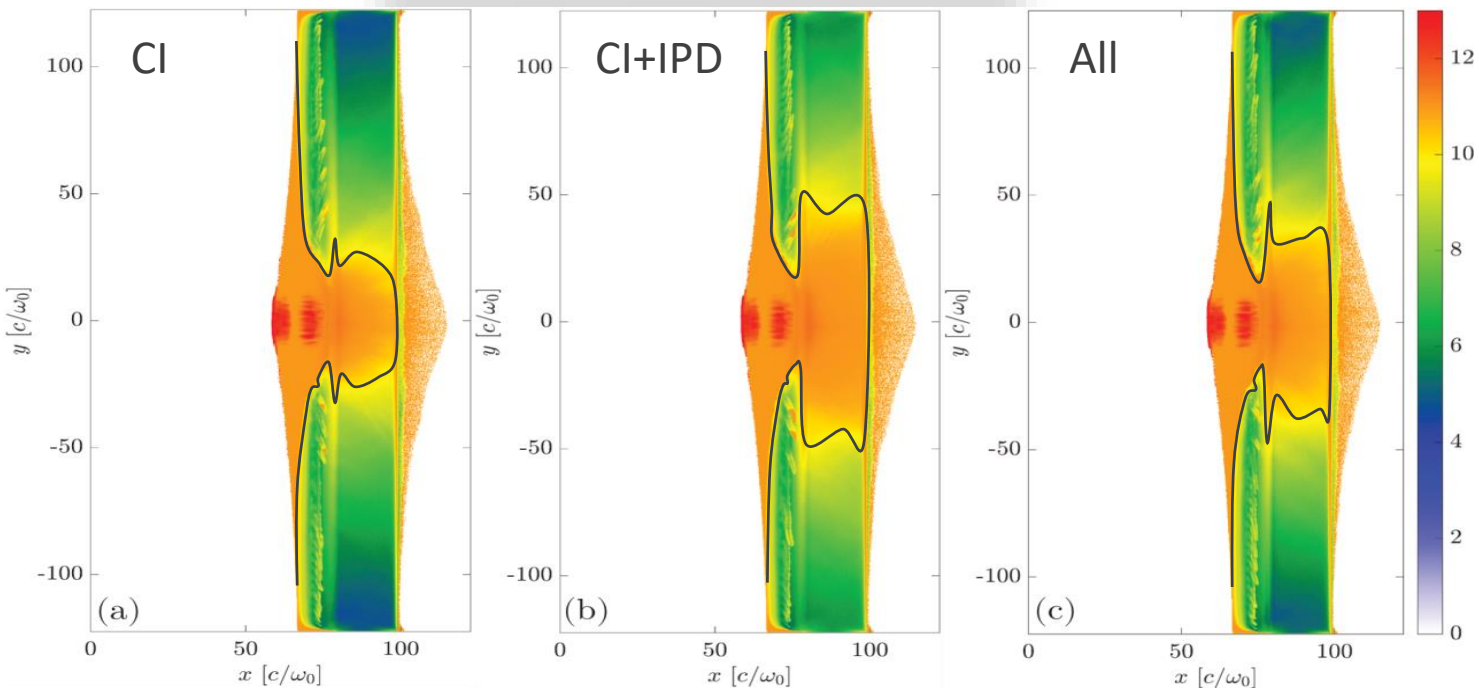

# Application to ultraintense laser-solid interactions

- Integrated simulation of a $1.36 \times 10^{20}\mathrm{Wcm}^{-2}$, 30 fs pulse with a 3 $\mu$m thick Al foil with a $\sim$ 2 $\mu$m scale length preplasma.
- Overall, accounting for all atomic physics processes leads to relatively weak changes to the heated target properties. However, compared to the CI only case, one obtains a significantly larger ionized region with slightly weaker ($\sim 0.5 - 1$ keV) temperatures.
- A clearer impact of the full atomic physics package is seen on the quasistatic magnetic fields generated by the fast electrons in the target as a result of resistive current filamentation.

*Quasistatic magnetic field $\langle B_z \rangle [10^4 T]$ at $t = 130\ fs$ after the laser maximum*

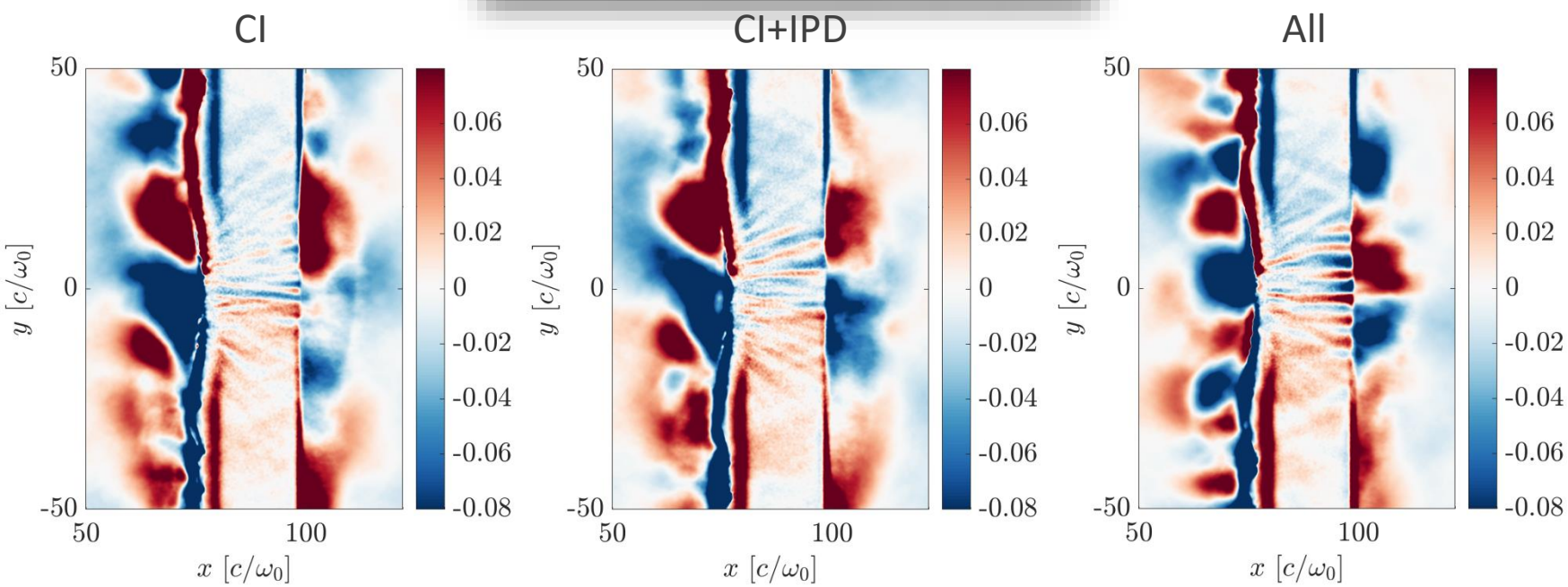

# PIC simulation of ultrafast heating of solid Al target by intense x-ray flashes

| $\rho$ | $T_{i0} = T_{e0}$ | $\Delta x = \Delta y$ | $\Delta t$ | $N_t$ | MP number/cell | $\frac{\langle p_{th} \rangle}{\Delta p_{xyz}}$ |
|---|---|---|---|---|---|---|
| 2.7 g/cm$^3$ | 5 eV | 4 nm | 5.31 as | 38 000 | 50 | 4 |

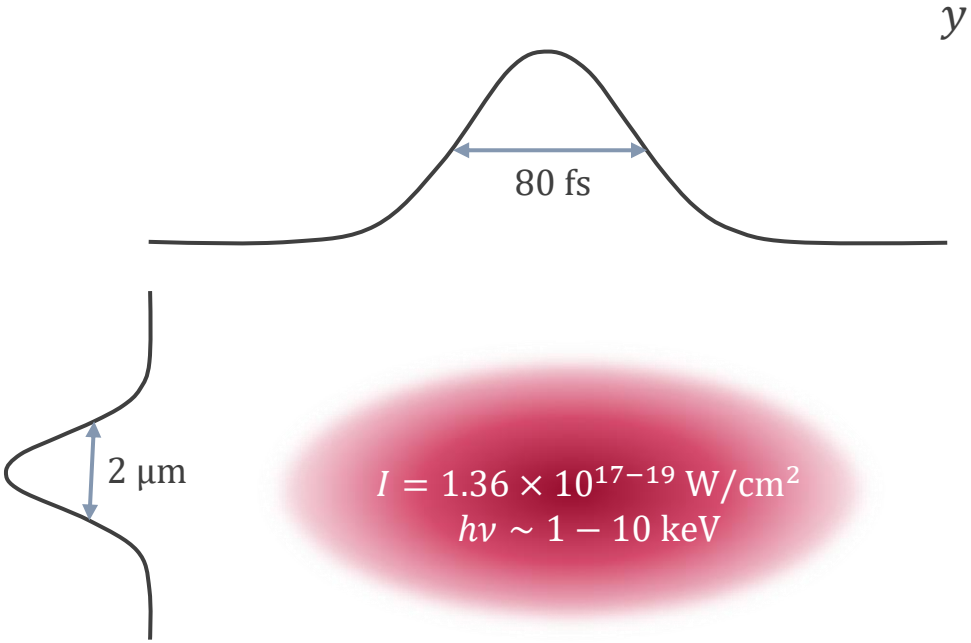


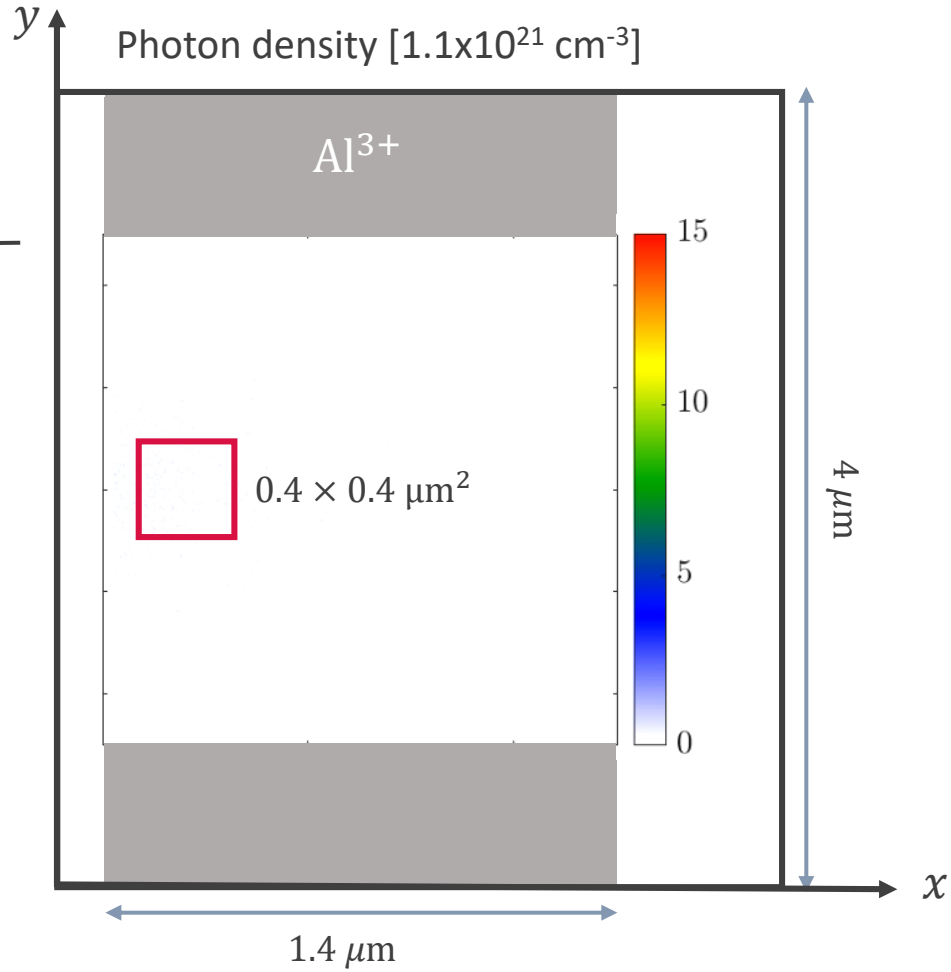


Simulation parameters similar to the PIC (PICLS) study of [Royle et al 2017][1]

[1]R. Royle *et al.*, Phys. Rev. E **95**, 063203 (2017).

# Case of $I = 1.36 \times 10^{17}\,\mathrm{Wcm^{-2}}$ and $h\nu = 1.7$ keV: Time evolution of electron energy distribution

**CALDER**

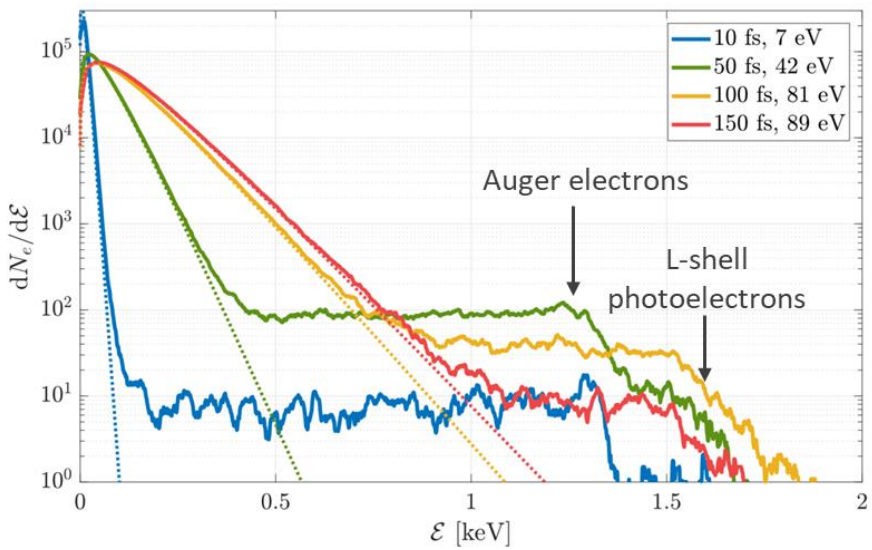


**PICLS[1]**

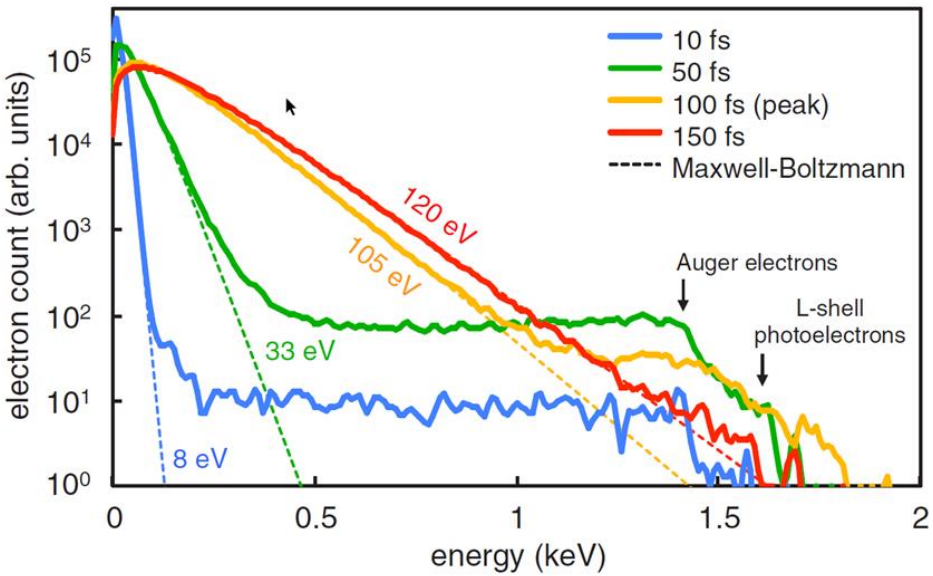


- The nonstationary electron energy spectrum comprises two distinct populations:
  - a suprathermal tail, filled by photoelectrons and KLL Auger electrons during the x-ray irradiation,
  - a Maxwellian bulk of time-increasing extent (from which the instantaneous electron temperature can be inferred) as suprathermal electrons thermalize via *e-e* collisions.
- CALDER and PICLS[1] results fairly agree, yet PICLS predicts a faster thermalization, attributed to different atomic physics models (Coulomb collisions, CI, TBR, IPD...).

[1]R. Royle *et al.*, Phys. Rev. E **95**, 063203 (2017).

# Nontrivial heating dynamics as a function of the x-ray photon energy ⇒ Existence of an optimum photon energy

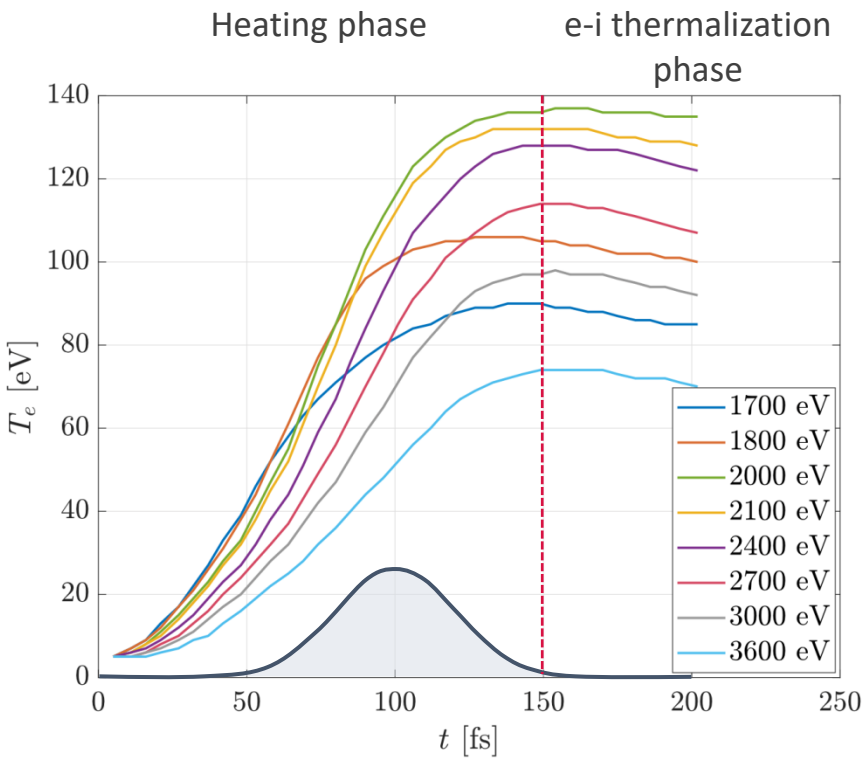


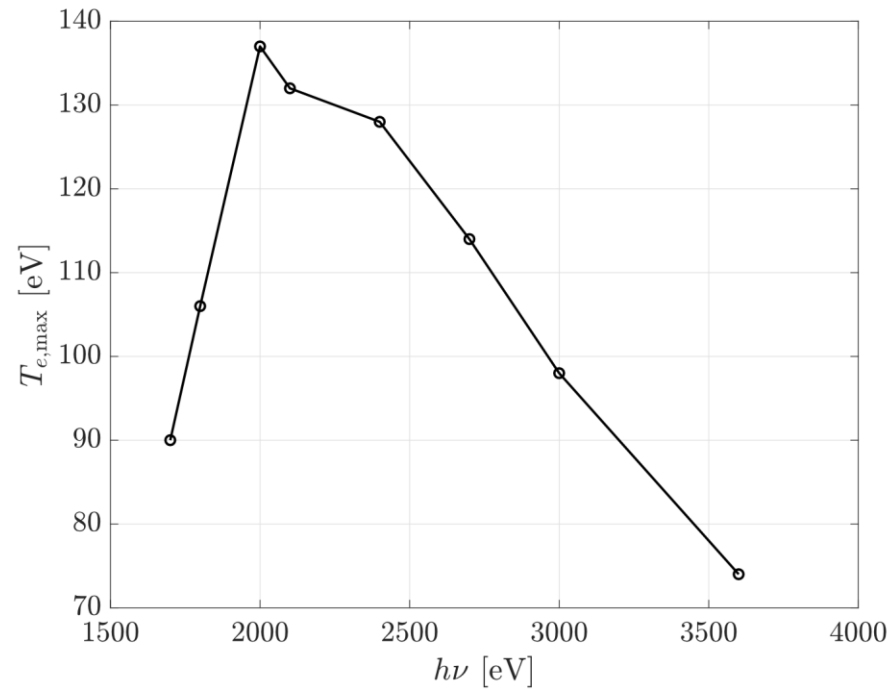


- Initial heating rate and saturation level depend on dynamic competition between productions of KLL Auger and photo-electrons.
- The rise in the K-shell binding energy with increasing $\langle Z^* \rangle$ can prematurely inhibit the production of KLL Auger electrons at low photon energies (e.g. at $h\nu = 1.7$ keV).
- At $I = 1.36 \times 10^{17} \mathrm{Wcm}^{-2}$, the maximum electron temperature ($T_{e,\max} \simeq 140$ eV) is obtained for $h\nu_{\mathrm{opt}} \simeq 2$ keV.
- At $I = 1.36 \times 10^{19} \mathrm{Wcm}^{-2}$, $T_{e,\max} \simeq 600$ eV and $h\nu_{\mathrm{opt}} \simeq 6$ keV.

# Conclusions and prospects

**Conclusions**

- CALDER now includes a comprehensive atomic physics package based on a fully PIC formalism.
- This new package has been successfully benchmarked against Saha-Boltzmann and FLYCHK models.
- CALDER has now the capability of computing x-ray emission spectra in a self-consistent way.
- Ultraintense and ultrashort laser-solid interactions show stronger influence of atomic physics on instability-driven magnetic-field generation.
- Ultrafast heating of Al samples by intense x-ray flashes as delivered by XFELs is predicted to be optimized at a specific photon energy, depending on the x-ray pulse intensity. This optimum results from the competition of Auger and photo-electrons.

**Prospects**

- Implement inverse Bremsstrahlung process, which may play a substantial role at ultrahigh x-ray pule intensities.
- Describe the finite relaxation time of atomic vacancies.

- Lever l'hypothèse d'instantanéité de la désexcitation atomique (au moins pour la couche K) en tenant compte des taux de relaxation[1].

- Implémentation du processus de Bremsstrahlung inverse dont les effets sur le chauffage peuvent être importants à très haut flux photonique[2].

- Tenir compte de l'IPD dans la photoionisation aussi pour la probabilité d'interaction (et pas seulement pour l'énergie du photo-électron).

- Amélioration du traitement de l'IPD en utilisant des modèles plus récents[3].

# Interprétation du taux de chauffage électronique initial

$I = 1.36$

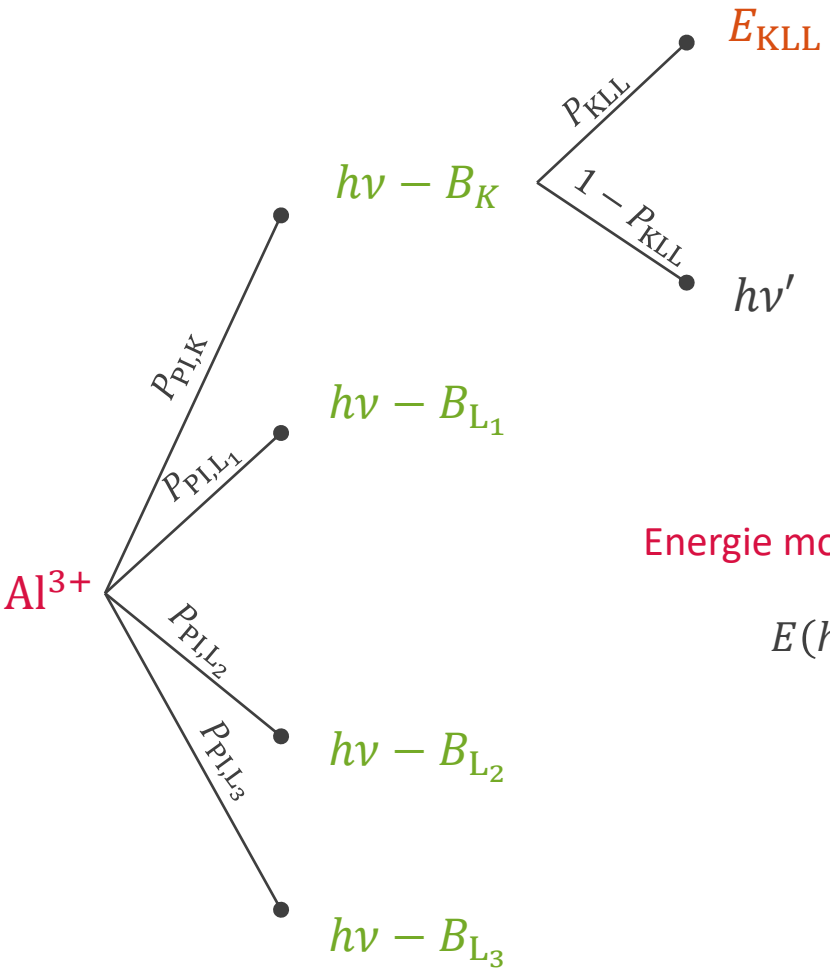


Energie moyenne :

$$
\begin{aligned}
E(h\nu) &= P_{\mathrm{PI,K}} P_{\mathrm{KLL}} E_{\mathrm{KLL}} \\
&+ P_{\mathrm{PI,K}}\,(h\nu - B_{\mathrm{K}}) \\
&+ P_{\mathrm{PI,L}_1}(h\nu - B_{\mathrm{L}_1}) \\
&+ P_{\mathrm{PI,L}_2}(h\nu - B_{\mathrm{L}_2}) \\
&+ P_{\mathrm{PI,L}_3}(h\nu - B_{\mathrm{L}_3})
\end{aligned}
$$

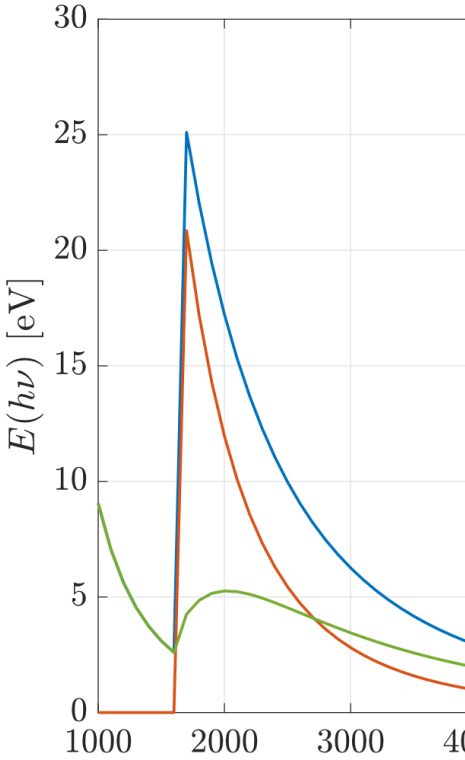


*Energie électronique m*
*des 10 premières fs*
*faisceau photonique.*

# Origine de l'optimum du chauffage électronique

$$I = 1.36 \times 10^{17}\ \mathrm{W/cm^2}$$

Compétition dynamique :

- Entre le chauffage par production d'électrons Auger ou de photo-électrons.
- Cette compétition entraine l'apparition d'un optimum vers $h\nu = 2000$ eV.
- Dans le cas de plus faible énergie photonique, décalage temporel entre le maximum de production d'énergie par les Auger et par les photo-électrons.

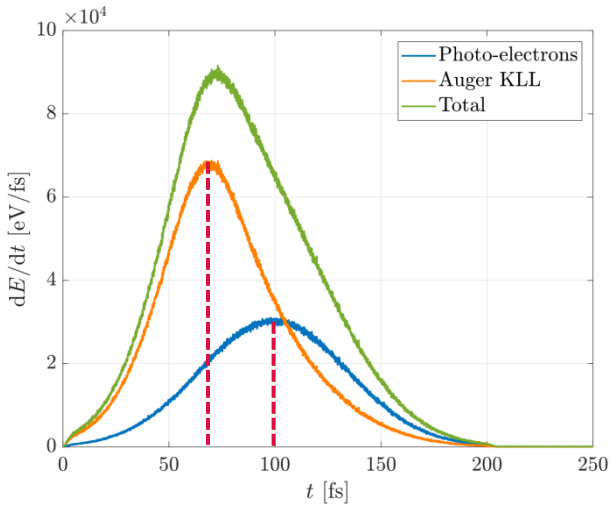


1700 eV

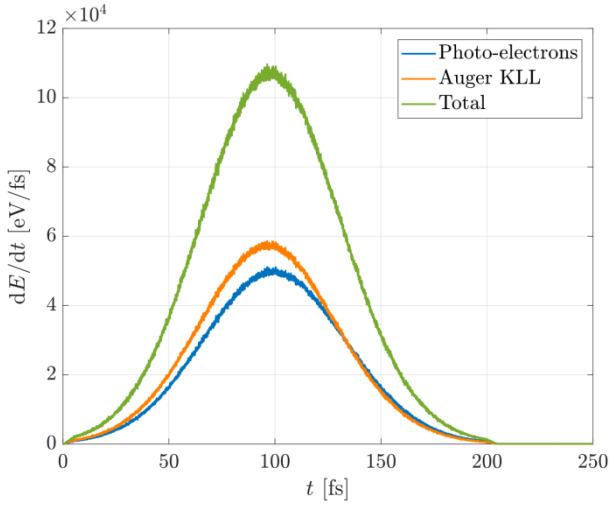


2400 eV

# Extinction prématurée de la production d'électrons Auger KLL à basse

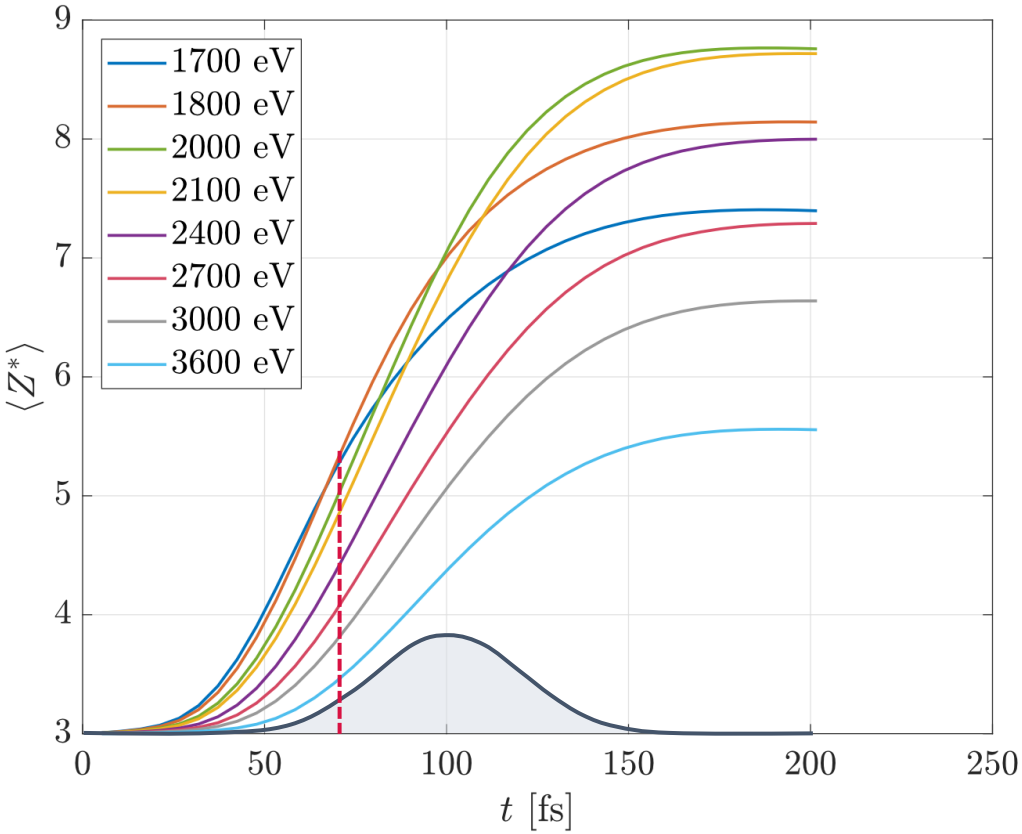


*Evolution temporelle de la charge ionique moyenne dans la simulation d'interaction XFEL-Al à* $I = 1.36 \times 10^{17}\ \mathrm{W/cm^2}$.

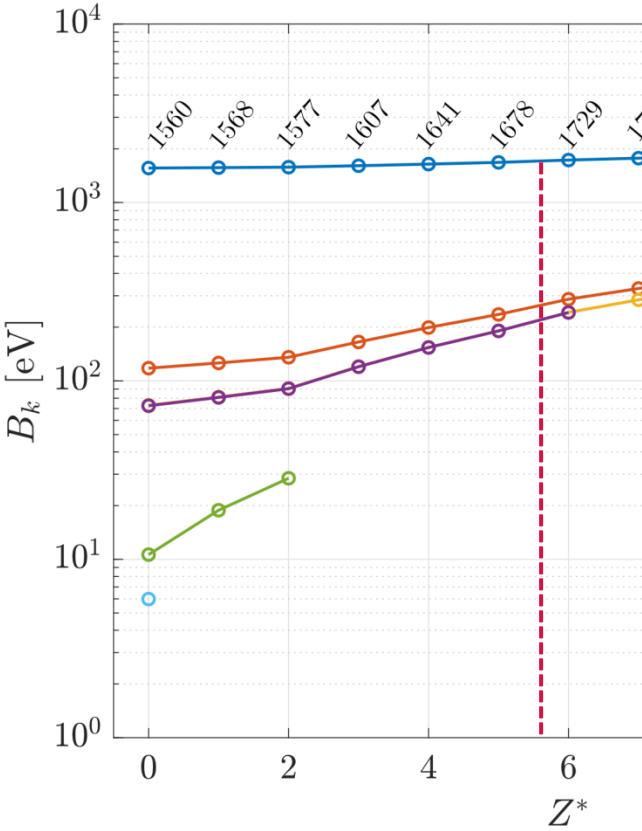


*Evolution des énergies de liai*
*en fonction de son état de char*

# Conclusions

- Implémentation d'un modèle quasi-complet de **physique atomique** et de **transport radiatif**.
- Validation de ces nouveaux modules : bonne reproduction des prédictions du **modèle de Saha** et du **FLYCHK**.
- Production de **spectres d'émission**.
- Nouveau système d'interaction accessible par CALDER : **XFEL-solide**. **Optimum du chauffage** él compétition dynamique entre production d'**électrons Auger** et de **photo-électrons**.
- Examen de l'effet de ces processus sur des grandeurs physiques macroscopiques dans un context Impact particulièrement visible sur les **fluctuations magnétiques**.